

Aeroelastic behavior of nano-composite beam-plates with double delaminations

S.B. Mousavi^a and Ali A. Yazdi*

Departement of Mechanical Engineering, Quchan University of Technology, P.O. Box 94717-84686, Quchan, Iran

(Received April 1, 2019, Revised October 31, 2019, Accepted November 14, 2019)

Abstract. In this paper aeroelastic behavior of 3-phase nano-composite beam-plate with double delaminations is investigated. It is tried to study the effect of carbon nano-tubes (CNTs) on critical flutter pressure of reinforced damaged nano-composite structures. In this case, the CNTs are appending to the polymer matrix uniformly. The Eshelby-Mori-Tanaka model is used to obtain the effective material properties of 3-phase nano-composite beam-plate. To investigate the aeroelastic behavior of delaminated beam-plate subjected to supersonic flow, it is assumed that the damaged segments are forced to vibrate together. The boundary conditions and auxiliary conditions at edges of delaminated segments are used to predict critical flutter pressure. The influence of CNTs and different delamination parameters such as delamination length, axial position and its position through thickness are investigated on critical flutter pressure.

Keywords: carbon nano-tubes; double delaminations; nano-composite; flutter

1. Introduction

The principle of improving overall performance of structures is not new, but appearance of new materials shows a significant improvement in many functional properties such as toughness and stiffness of structures. Carbon nano-tubes (CNTs) materials due to their high electrical conductivity, tensile strength, thermal conductivity and flexibility have been persuaded researchers to investigate their effects in design of functional nano-composites structures. The molecular dynamic simulation (MDS) and continuum models are two effective methods to model the mechanical behaviors of nano-materials (Hu *et al.* 2012). Shi *et al.* (2017) used first-order shear deformation (FSDT) theory to investigate analytically free vibration of functionally-graded carbon nanotubes (FGCNTs) reinforced composite beams. Zhang *et al.* (2017) considered the effects of rotary inertia and transverse shear deformation on vibration behavior of moderately thick FGCNTs reinforced composite quadrilateral plates resting on elastic foundation. In this study, influence of different effective parameters such as CNT ratio, distributions through thickness, boundary conditions and fiber angles were considered.

Mehar and Panda (2016) employed different plate theories with finite element method to study free vibration and bending behavior of CNTs reinforced composite (CNTRC) panels under thermal effects numerically. According to this study, increasing CNTs volume fraction

can improve non-dimensional fundamental frequency. Rafiee *et al.* (2014a, b) studied nonlinear vibration of CNTRC plates due to existence of different mechanical and thermal loads under the effect of piezoelectric layers on frequency ratios. According to the results, the nonlinear response is function of CNTs volume fraction, piezoelectric material voltage and thickness. Ribeiro (2016) used arc-length continuation and harmonic balance methods to investigate nonlinear vibration of CNTs under effects of electrostatic forces. In this study, the geometrical and local effects on nonlinear behavior and natural frequencies were considered.

Tornabene *et al.* (2017) used FSDT to formulate the governing equations of nano-composite plates and shells. Additionally, they used generalized differential quadrature (GDQ) method to study free vibration numerically. In this study, CNTs were used to improve the polymer matrix mechanical properties. The Mori-Tanaka model was utilized to obtain the CNTs density in the matrix. In this study, the effect of CNTs mass fraction and agglomeration were considered. Seidi and Kamarian (2017) investigation illustrated effect of CNTs on free vibration of multi-scale nano-composite beams. The effective materials properties of the laminated reinforced nano-composite beam were obtained based on Mori-Tanaka model. The GDQ method was used to solve the governing equation of the system.

He *et al.* (2015) used a fractional-order time derivative model to investigate large amplitude free and force vibration of CNTs/fiber/polymer multiscale nano-composite beams. Based on the results of this study, nonlinear frequencies and frequency-amplitude relationship were function of viscoelastic damping coefficient. Rafiee *et al.* (2016) developed a computational model to study nonlinear response of rotating cantilever thin-walled CNTs/fiber/polymer multiscale nano-composite blades. According to

*Corresponding author, Ph.D., Assistant Professor,

E-mail: aliaminyazdi@qiet.ac.ir

^a M.Sc. Student

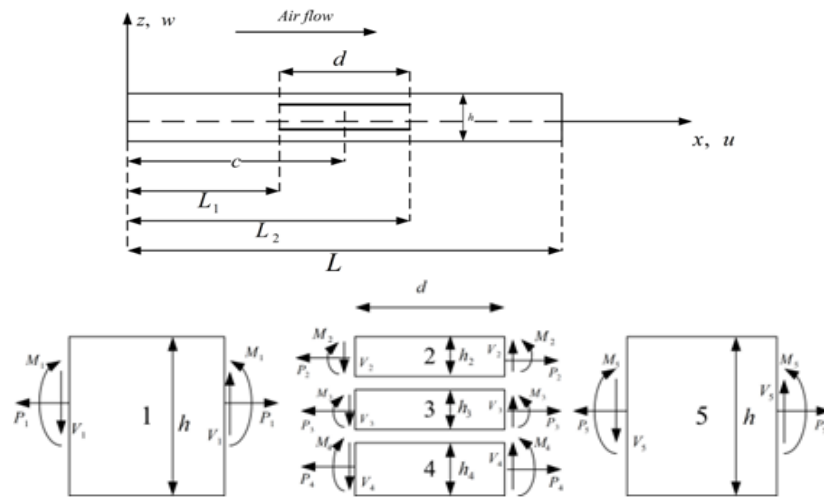


Fig. 1 Beam-plate geometric parameters

the results, the natural frequencies of multiscale nano-composite beams and blades are dependent on CNTs mass fraction, significantly. Additionally, it was shown that SWCNTs are more capable to affect nonlinear response and frequency of multiscale nano-composite beams in comparison to the multi-walled carbon nanotubes (MWCNTs).

The CNTs particle can be the best candidate to improve the delamination resistance properties of damaged composites structures. Gojny *et al.* (2004) investigation had shown the effect of addition double wall CNTs on toughness property of epoxy resin. According to this study, nano-composite structure had remarkably higher fracture toughness in comparison to the neat epoxy. Zheng *et al.* (2017) studied the applicability of CNTs to increase the inter-laminar fracture toughness in delaminated carbon fibers/epoxy composite.

Tsanyzalis *et al.* (2007) study described effect of zirconate titanate and carbon nano-tube fiber (CNF) on fracture toughness of carbon fiber reinforced plastic (CFRP) laminates. According to the results of this study, addition of only 1% CNF in matrix yields 100% increase of fracture toughness in Mode I.

Kim *et al.* (2008) studied the effect of MWCNTs on delamination resistance property of CFRP. It had been shown that adding 0.2 and 0.7 weight percentage of MWCNTs into the matrix yields inter-laminar fracture toughness improvement of Mode I at the cryogenic temperature. Additionally, Ozdemir *et al.* (2016) reported that addition of 0.2% of rubber particles into the epoxy matrix results 250% increase of delamination resistance. Kepple *et al.* (2008) studied preparation of woven carbon fiber with CNTs to consider the effect of nanotubes growth on carbon fiber. The results of this study depicted that the laminate delamination resistance can increase up to 50% with grown nanotubes. Additionally, it was shown that CNTs can affect flexural modulus and improve it up to 5%. Alidoost and Rezaeepazhand (2017) used classical laminate and Euler-Bernoulli beam theories to investigate buckling, vibration and flutter of damaged composite beam under effect of follower force.

Tracy and Pardoen (1989) used analytical and experimental methods to investigate the effect of delamination on natural frequencies of composite beam. Murugan *et al.* (2013) investigated aeroelastic response of composite helicopter rotor. In this study the elastic modulus and Poisson's ratio were considered as variable parameters.

Yazdi and Rezaeepazhand (2012) extended the applicability of similitude theory to obtain the aeroelastic instability boundaries of delaminated plates. Shishesaz *et al.* (2017) developed a FEM model to consider the influence of circular damaged area on crack growth of composite plate. Based on the results obtained, the first opening mode plays significant role in delamination process.

Rafiee *et al.* (2017) reviewed investigations including analytical, semi-analytical and numerical methods to design rotating composite beams and blades. In this investigation, the governing equations of the system were used to obtain the scaling laws. Moreover, Yazdi (2012) studied the aeroelastic instability of symmetric delaminated cylindrical shells. The governing equations were obtained based on the assumptions of Love's shell theory and von Karman-Donnell kinematic relations. Additionally, Galerkin method was used to obtain the flutter pressure of delaminated cylindrical shell.

The main aim of this study is to consider the application of CNTs fillers in the polymer matrix to improve the flutter boundary of composite beam-plates with double delaminations. In this case, mechanical properties of traditional polymer matrix composite are improved by adding a small amount of CNTs into the polymer matrix. The Mori-Tanaka model is used to formulate the material properties of reinforced nano-composite beam-plates. To illustrate the problem, two-width delaminations as shown in Fig. 1 are considered. The delaminated beam-plate is divided into five segments; delamination segments and two un-delaminated regions. The equation of motion for each segment are formulated and by imposing the boundary conditions at the ends of un-delaminated segments and continuity conditions at delamination junctions, the critical flutter boundary of delaminated 3-phase nano-composite beam-plate are obtained.

2. Problem formulation

The governing equations for delaminated beam-plates with double delaminations subjected to supersonic flow parallel to the plate length are as follow (Tracy and Pardeon 1989)

$$D_1 \frac{\partial^4 w_1}{\partial x^4} + \rho_c h \frac{\partial^2 w_1}{\partial t^2} + \Delta P = 0 \quad (1a)$$

$$\left(D_2 - \frac{B_2^2}{A_2}\right) \frac{\partial^4 w_2}{\partial x^4} - P_2 \frac{\partial^2 w_2}{\partial x^2} + \rho_c h_2 \frac{\partial^2 w_2}{\partial t^2} + \Delta P + F_2 = 0 \quad (1b)$$

$$\left(D_3 - \frac{B_3^2}{A_3}\right) \frac{\partial^4 w_3}{\partial x^4} - P_3 \frac{\partial^2 w_3}{\partial x^2} + \rho_c h_3 \frac{\partial^2 w_3}{\partial t^2} + F_3 = 0 \quad (1c)$$

$$\left(D_4 - \frac{B_4^2}{A_4}\right) \frac{\partial^4 w_4}{\partial x^4} - P_4 \frac{\partial^2 w_4}{\partial x^2} + \rho_c h_4 \frac{\partial^2 w_4}{\partial t^2} + F_4 = 0 \quad (1d)$$

$$D_5 \frac{\partial^4 w_5}{\partial x^4} + \rho_c h \frac{\partial^2 w_5}{\partial t^2} + \Delta P = 0 \quad (1e)$$

where F_i is the contact forces between the delaminated segments, P_i is the in-plane forces induced due to delaminations, ρ_c is the density of reinforced beam-plates and ΔP is the aerodynamic pressure. To evaluate the aerodynamic pressure, the piston aerodynamic theory is used

$$\Delta P = -\frac{\rho U^2}{\sqrt{M^2 - 1}} \left[\frac{\partial w}{\partial x} + \frac{1}{U} \frac{M^2 - 2}{M^2 - 1} \frac{\partial w}{\partial t} \right] = \lambda \frac{\partial w}{\partial x} + g \frac{\partial w}{\partial t} \quad (2)$$

Considering Euler-Bernoulli's beam theory, the only nontrivial strain for the i -th segment is as follow

$$\varepsilon_{xx}^i = \frac{\partial u_i}{\partial x} - z_i \frac{\partial^2 w_i}{\partial x^2} \quad i = 1, 2, 3, 4, 5 \quad (3)$$

where u and w are the displacement components and are function of x and t . Based on this fact, the axial load acting on segment i is given as follow

$$P_i = \int_{h_{k-1}}^{h_k} \int_{A_i} (\bar{Q}_{11})_k \left(\frac{\partial u_i}{\partial x} - z_i \frac{\partial^2 w_i}{\partial x^2} \right) dA_i dz, \quad (4)$$

$$P_i = A_i \frac{\partial u_i}{\partial x} - B_i \frac{\partial^2 w_i}{\partial x^2} \quad i = 2, 3, 4$$

where \bar{Q}_{11} is the transferred reduced stiffness coefficient, h_k is the z -coordinate of the surface of the k -th layer and

$$A_i, B_i, D_i = \int_{h_{k-1}}^{h_k} (\bar{Q}_{11})_k (1, z, z^2) dz \quad (5)$$

As it is mentioned, the aim of this study is to investigate the aeroelastic behavior of multi-scale nano-composite delaminated beam plates subjected to supersonic flow. In this case the polymer matrix is reinforced by CNTs uniformly and then the fibers are embedded in the matrix. For perfect distribution and impregnation with polymer, the following equation can be used for elastic modulus of nano-composite (Rafiee *et al.* 2014b)

$$E_{NC} = \frac{3}{8} \left\{ 1 + 2 \left(\frac{l}{d} \right) \left[\frac{\left(\frac{E_{CNT}}{E_m} \right) - \left(\frac{d_{CNT}}{4t} \right)}{\left(\frac{E_{CNT}}{E_m} \right) + \left(\frac{l_{CNT}}{2t} \right)} \right] V_{CNT} \right\} \\ \times \left\{ 1 - \left[\frac{\left(\frac{E_{CNT}}{E_m} \right) - \left(\frac{d_{CNT}}{4t} \right)}{\left(\frac{E_{CNT}}{E_m} \right) + \left(\frac{l_{CNT}}{2t} \right)} \right] V_{CNT} \right\}^{-1} E_m \quad (6)$$

$$+ \frac{5}{8} \left\{ 1 + 2 \left[\frac{\left(\frac{E_{CNT}}{E_m} \right) - \left(\frac{d_{CNT}}{4t} \right)}{\left(\frac{E_{CNT}}{E_m} \right) + \left(\frac{l_{CNT}}{2t} \right)} \right] V_{CNT} \right\} \\ \times \left\{ 1 - \left[\frac{\left(\frac{E_{CNT}}{E_m} \right) - \left(\frac{d_{CNT}}{4t} \right)}{\left(\frac{E_{CNT}}{E_m} \right) + \left(\frac{l_{CNT}}{2t} \right)} \right] V_{CNT} \right\}^{-1} E_m$$

where E_m is elastic modulus of polymer matrix (2.27×10^9 Kg/m²), E_{CNT} is elastic modulus (640×10^9 kg/m²), l_{CNT} is the length (25×10^{-6} m), d_{CNT} is the diameter (1.4×10^{-9} m) and t is the thickness of SWCNTs (0.34×10^{-9} m), respectively. The volume fraction (V_{CNT}) of CNTs can be expressed in terms of CNTs weight percentage (ω_{CNT}) and mass density of polymer matrix ($\rho_m = 1200$ kg/m³) and CNTs ($\rho_{CNT} = 1350$ kg/m³) as follow

$$V_{CNT} = \frac{\omega_{CNT}}{\omega_{CNT} + (\rho_{CNT}/\rho_m) - (\rho_{CNT}/\rho_m)\omega_{CNT}} \quad (7)$$

Due to the random distribution of CNTs in the polymer matrix, the isotropy assumption can be used and the shear modulus is defined as (Tornabene *et al.* 2017)

$$G_{NC} = \frac{E_{NC}}{2(1 + \nu)} \quad (8)$$

$$\nu_{NC} = \nu_m \quad (9)$$

Now, using the rule of mixture the effective material properties of 3-phase nano-composite materials are achieved (Seidei and Kamarian 2017)

$$E_{11} = V_f E_f + V_{NC} E_{NC} \quad (10)$$

$$\frac{1}{E_{22}} = \frac{V_f}{E_f} + \frac{V_{NC}}{E_{NC}} - V_f E_{NC} \frac{v_f^2 \frac{E_{NC}}{E_f} + v_{NC}^2 \frac{E_f}{E_{NC}} - 2v_f v_{NC}}{V_f E_f + V_{NC} E_{NC}} \quad (11)$$

$$\frac{1}{G_{12}} = \frac{V_f}{G_f} + \frac{V_{NC}}{G_{NC}} \quad (12)$$

$$\nu_{12} = V_f \nu_f + V_{NC} \nu_{NC} \quad (13)$$

$$\rho_{NC} = V_{NT} \rho_{NT} + V_m \rho_m \quad (14)$$

According to the classical plate theory and under effect of small deflections, the transferred reduced stiffness matrix is given as follow

$$\begin{bmatrix} \bar{Q}_{11} & \bar{Q}_{12} & \bar{Q}_{16} \\ \bar{Q}_{12} & \bar{Q}_{22} & \bar{Q}_{26} \\ \bar{Q}_{16} & \bar{Q}_{26} & \bar{Q}_{66} \end{bmatrix} = \begin{bmatrix} C^2 \theta & S^2 \theta & 2S\theta C\theta \\ S^2 \theta & C^2 \theta & -2S\theta C\theta \\ -S\theta C\theta & S\theta C\theta & C^2 \theta - S^2 \theta \end{bmatrix}^{-1} \quad (15)$$

$$\begin{bmatrix} E_{11} & v_{12}E_{11} & 0 \\ 1-v_{12}v_{21} & 1-v_{12}v_{21} & 0 \\ v_{12}E_{11} & E_{22} & 0 \\ 1-v_{12}v_{21} & 1-v_{12}v_{21} & 0 \\ 0 & 0 & G_{12} \\ C^2\theta & S^2\theta & 2S\theta C\theta \\ S^2\theta & C^2\theta & -2S\theta C\theta \\ -S\theta C\theta & S\theta C\theta & C^2\theta - S^2\theta \end{bmatrix} \quad (15)$$

where $C\theta = \cos \theta$ and $S\theta = \sin \theta$. Due to the nonlinear nature of contact force (F) between delaminated segments in Eq. (1), it is assumed that the delaminated parts are forced to vibrate together. Base on this fact, the nonlinear term can be neglected (Alidoost and Rezaeepazhand 2017). It should be noted that the beam-plate is not under effect of any axial loads at it ends ($P_1 = P_5 = 0$) and in result $P_1 = P_2 + P_3 + P_4 = 0$. According to these facts, Eq. (1) can be written as

$$D_1 \frac{\partial^4 w_1}{\partial x^4} + \rho_c h \frac{\partial^2 w_1}{\partial t^2} + \Delta P = 0 \quad (16a)$$

$$\bar{D}_2 \frac{\partial^4 w_2}{\partial x^4} + \rho_c h \frac{\partial^2 w_2}{\partial t^2} + \Delta P = 0 \quad (16b)$$

$$D_5 \frac{\partial^4 w_5}{\partial x^4} + \rho_c h \frac{\partial^2 w_5}{\partial t^2} + \Delta P = 0 \quad (16c)$$

$$\bar{D}_2 = D_2 + D_3 + D_4 - \frac{B_2^2}{A_2} - \frac{B_3^2}{A_3} - \frac{B_4^2}{A_4} \quad (16d)$$

For each segment, the displacement in z -direction can be formulated as $w_i = W_i(x) e^{j\omega t}$. Substituting the assuming solution into Eq. (16) yields

$$\bar{D}_i \frac{d^4 W_i}{dx^4} + \lambda \frac{dW_i}{dx} + (j\omega g - \omega^2) W_i = 0 \quad (17)$$

$i = 1, 2, 5, \quad j = \sqrt{-1}$

The solution of Eq. (17) is as (Tracy and Paderon 1989)

$$W_i(x) = C_{1i} e^{s_{1i}x} + C_{2i} e^{s_{2i}x} + C_{3i} e^{s_{3i}x} + C_{4i} e^{s_{4i}x}, \quad (18)$$

$i = 1, 2, 5$

where S_{ni} ($n = 1, 2, 3, 4$) are the roots of characteristic equation of each segment. Solving Eq. (18) for multi-scale (3-phase) nano-composite delaminated beam-plates requires 12 boundary conditions. The boundary conditions for delaminated beam-plate at its ends provide four conditions. For simply supported boundary conditions at the ends of beam-plate one can write

$$x = 0 : \quad w_1(0) = \frac{\partial^2 w_1(0)}{\partial x^2} = 0 \quad (19a)$$

$$x = L : \quad w_5(L) = \frac{\partial^2 w_5(L)}{\partial x^2} = 0 \quad (19b)$$

Additionally, auxiliary conditions at the edges of delaminated segments can provide 8 boundary conditions are necessary for obtaining the flutter boundary of delaminated multi-scale (3-phase) nano-composite beam

plate

$$x = L_1 : \quad w_1(L_1) = w_2(L_1), \quad \frac{\partial w_1(L_1)}{\partial x} = \frac{\partial w_2(L_1)}{\partial x} \quad (20)$$

$$x = L_2 : \quad w_2(L_2) = w_5(L_2), \quad \frac{\partial w_2(L_2)}{\partial x} = \frac{\partial w_5(L_2)}{\partial x} \quad (21)$$

$$x = L_1 : \quad V_1 = V_2 + V_3 + V_4, \quad M_1 = M_2 + M_3 + M_4 \quad (22)$$

$$x = L_2 : \quad V_5 = V_2 + V_3 + V_4, \quad M_5 = M_2 + M_3 + M_4 \quad (23)$$

where V_i and M_i are the shear force and bending moment and can be defined as follow

$$M_i = \int_{h_{k-1}}^{h_k} \int_{A_i} (\bar{Q}_{11})_k \left(\frac{\partial u_i}{\partial x} - z_i \frac{\partial^2 w_i}{\partial x^2} \right) dA_i z \, dz \quad (24a)$$

$$M_i = B_i \frac{\partial u_i}{\partial x} - D_i \frac{\partial^2 w_i}{\partial x^2} \quad (24b)$$

$$V_i = - \left(D_i - \frac{B_i^2}{A_i} \right) \frac{\partial^3 w_i}{\partial x^3} \quad (24c)$$

Using Eqs. (24) and (4), it can be written

$$M_i = \frac{B_i P_i}{A_i} - \left(D_i - \frac{B_i^2}{A_i} \right) \frac{\partial^2 w_i}{\partial x^2}, \quad i = 1, 2, 5 \quad (25)$$

By using Eq. (4) through delamination length the averages of axial forces of axial forces appear due to delamination can be obtained

$$\frac{P_2}{A_2}(x)_{L_1}^{L_2} = \Delta u_{x=L_1}^{x=L_2} - \frac{B_2}{A_2} \left(\frac{\partial^2 w_2}{\partial x^2} \right)_{x=L_1}^{x=L_2} \quad (26a)$$

$$\frac{P_3}{A_3}(x)_{L_1}^{L_2} = \Delta u_{x=L_1}^{x=L_2} - \frac{B_3}{A_3} \left(\frac{\partial^2 w_3}{\partial x^2} \right)_{x=L_1}^{x=L_2} \quad (26b)$$

$$\frac{P_3}{A_3}(x)_{L_1}^{L_2} = \Delta u_{x=L_1}^{x=L_2} - \frac{B_3}{A_3} \left(\frac{\partial^2 w_3}{\partial x^2} \right)_{x=L_1}^{x=L_2} \quad (26c)$$

Additionally, $P_2 + P_3 + P_4 = 0$, in this case we have

$$P_2 = \frac{B_4 A_2 + B_3 A_2 - B_2 A_4 - B_2 A_3}{(A_2 + A_3 + A_4)(L_2 - L_1)} \quad (27a)$$

$$P_3 = \frac{B_4 A_2 + B_2 A_3 - B_3 A_2 - B_3 A_4}{(A_2 + A_3 + A_4)(L_2 - L_1)} \quad (27b)$$

$$P_4 = \frac{B_2 A_4 + B_3 A_4 - B_4 A_2 - B_4 A_3}{(A_2 + A_3 + A_4)(L_2 - L_1)} \quad (27c)$$

Now using the mentioned boundary and axillary conditions and also use Eqs. (27) a matrix equation is obtained

Table 1 Comparison of three natural frequency of delaminated beam-plates with Tracy and Paderon (1989)

Delamination length (d/L)	Natural frequency(Hz)					
	Mode I		Mode II		Mode III	
	This study	(Tracy and Paderon 1989)	This study	(Tracy and Paderon 1989)	This study	(Tracy and Paderon 1989)
0	1	1	1	1	1	1
0.1	1	1	0.995	0.992	0.993	1
0.2	0.998	0.998	0.962	0.952	0.988	0.99
0.3	0.996	0.996	0.894	0.871	0.957	0.958
0.4	0.984	0.99	0.802	0.774	0.884	0.87
0.5	0.975	0.98	0.711	0.689	0.776	0.767
0.6	0.964	0.97	0.653	0.635	0.7	0.688
0.7	0.952	0.956	0.612	0.6	0.652	0.644
0.8	0.932	0.93.3	0.595	0.584	0.628	0.622
0.9	0.899	0.896	0.584	0.573	0.623	0.619
1	0.852	0.85	0.582	0.57	0.621	0.615

$$[K]_{12 \times 12} \{C\}_{12 \times 1} = \{0\}_{12 \times 1} \quad (28)$$

where $\{C\}$ is the vector of unknown parameters and $[K]$ is the matrix of coefficients. To calculate flutter pressure of delaminated reinforced composite beam-plate, it is necessary to set the determinant of coefficient matrix equal zero. In the next section, the effects of different parameters are discussed on critical flutter boundary of multi-scale nano-composite beam plates in details.

3. Results and discussions

In this study, the non-dimensional flutter pressure and its Eigen-value are defined as follow

$$\lambda_{ND} = \frac{\lambda L^3}{D_0} \quad (29)$$

$$Z = \pi^4 \left[ig \frac{\omega}{\omega_0} - \left(\frac{\omega}{\omega_0} \right)^2 \right] \quad (30)$$

Table 1 shows the accuracy of the presented method in this study. In this table, the frequencies ratio are compared with data of (Tracy and Pardeon 1989). According to this table the obtained results show good agreement with (Tracy and Pardeon 1989).

Figs. 2 and 3 depicted the effect of delamination length on flutter pressure of four layers uni-directional and cross-ply delaminated beam-plates, respectively. As it can be seen, for larger values of delamination length ($d/L > 0.2$), as result of increasing delaminations, the critical flutter pressure is dropped 50% approximately. It is also observed that, due to increasing the distance between two delaminations, the non-dimensional flutter pressure is also increased. In Fig. 4 the effect of delamination axial position on flutter pressure is shown.

As delaminations approach the two ends of the beam-plate, the critical flutter pressure increases. These changes have greater effect on smaller values of delamination length.

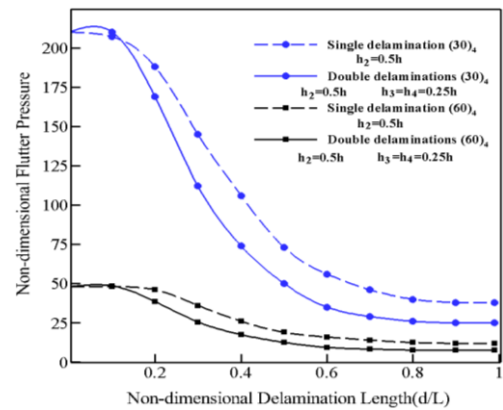


Fig. 2 Effect of delamination length on non-dimensional flutter pressure of four layers unidirectional delaminated beam-plates ($c/L = 0.5$)

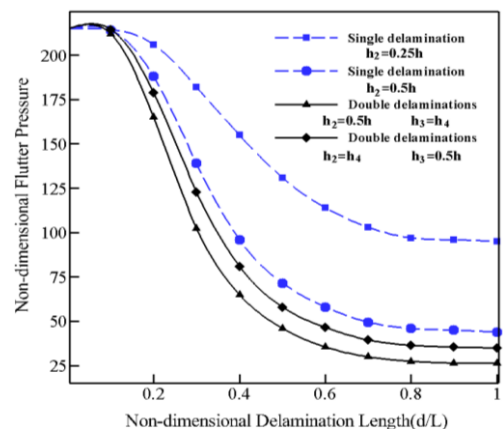


Fig. 3 Effect of delamination length on non-dimensional flutter pressure of symmetric cross-ply $(0/90)_s$ composite delaminated beam-plates ($c/L = 0.5$)

In other words, if the boundary conditions at edges of delamination are more restricted then flutter pressure is increased.

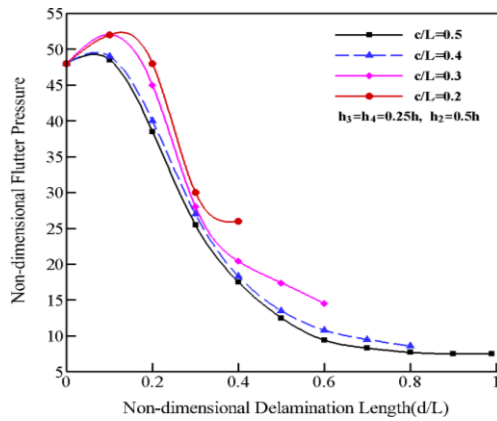


Fig. 4 Effect of delamination axial position and length on non-dimensional flutter pressure of four layers unidirectional $(60)_4$ composite delaminated beam-plates with double delaminations ($c/L = 0.5$)

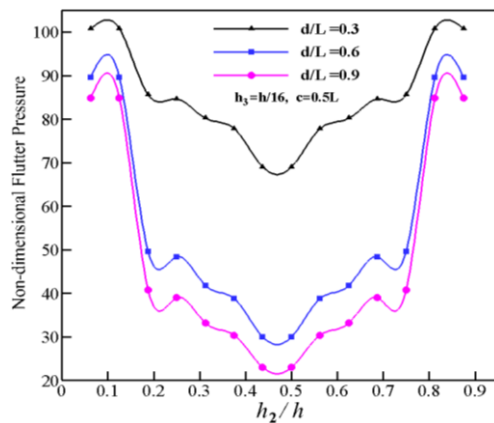


Fig. 5 Flutter pressure variation with delamination location through thickness symmetric quasi-isotropic $(90/\pm 45/0)_{2S}$, $c/L = 0.5$

Fig. 5 shows the effect of delamination position along thickness on flutter boundary of 16 layers symmetric quasi-isotropic delaminated beam-plates with double delaminations. As it is shown, the distance between two delaminations is constant ($h_3 = 0.0625 h$). In this case, by approaching the midpoint of distance between two delaminations to mid-plane of the beam-plates, the flutter critical pressure is decreased considerably. Additionally, it should be noted that the delamination length plays a significant role in this variation.

In Fig. 6 the distance between delaminated segments (h_3) does not remain constant. It should be noted that the position of the two delaminated segments changes symmetrically relative to the mid-plane. By reducing the distance between two delaminated segments, the critical flutter pressure also decreases. In other words, as long as two delaminated move toward the top and bottom surfaces of the beam, flutter pressure increases.

Fig. 7 depicted variation of eigenvalue with dynamic pressure for unidirectional beam-plate with two delaminations. As it can be seen, by increasing velocity of air flow over delaminated beam-plates two vibration modes

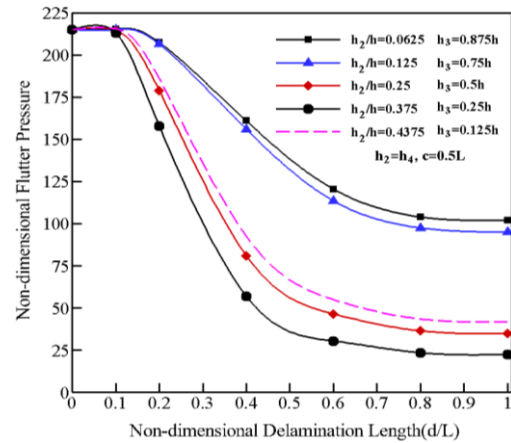


Fig. 6 Variation of flutter pressure with delamination position through thickness for $(0/90)_{4S}$

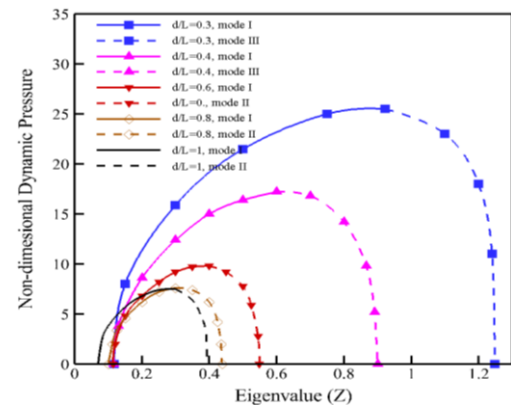


Fig. 7 Variation of dynamic pressure with eigenvalue for $(60)_4$

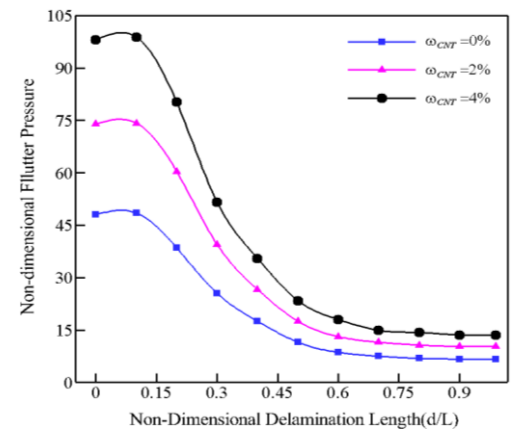


Fig. 8 Effects of CNTs on flutter pressure of four layers unidirectional $(60)_4$ delaminated beam-plates with double delaminations ($c/L = 0.5$, $h_2/h = 0.5$, $h_3 = h_4$)

of delaminated composite beam-plates merge to each other. Once these modes are close to each other the flutter pressure is obtained. According to this figure, for lower value of delamination length mode I and III are merged to each other while by enlarging delamination length this behavior changes completely and mode I and II will get close.

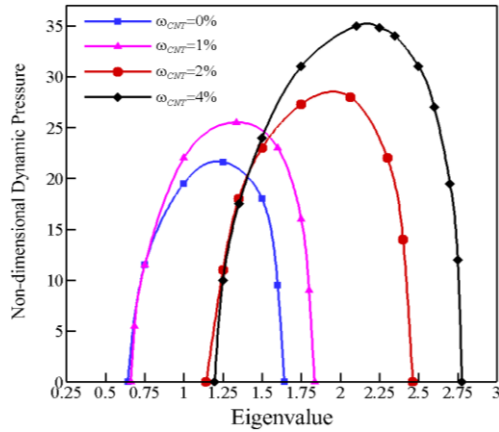


Fig. 9 Variation of dynamic pressure with eigenvalue for CNTs reinforced composite beam-plate with double delaminations $(0/90)_S$ ($h_3 = h_4 = 0.25h$, $d/L = 0.6$)

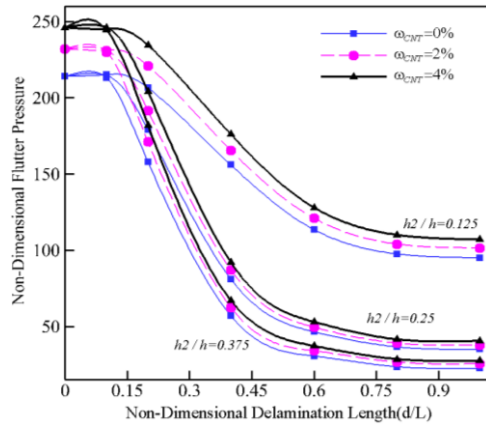


Fig. 10 Effect of delamination length on flutter pressure of delaminated cross-ply beam-plate with double delamination reinforced with CNTs $(0/90)_{4S}$ ($h_3/h = 1/16$, $c/L = 0.5$)

In Fig. 8 effect of CNTs on flutter pressure of delaminated reinforced unidirectional composite beam-plates is shown. According to this figure, adding only 4% CNTs can result 95% increase on flutter pressure of composite delaminated beam-plates. In other words, adding 4% CNTs can improve 72% the elastic modulus of reinforced composite delaminated beam-plates. This behavior can be observed from the frequency coalescence plot depicted in Fig. 9. According to the result for neat epoxy and 1% CNTs reinforced delaminated cross-ply beam-plates, the flutter pressure will occur between modes 1 and 2 while for 2 and 4 percent CNTs reinforced nano-composite delaminated beam-plates the frequency coalescence shifts to modes 2 and 4. In Figs. 10 and 11 the effect of CNTs on flutter pressure variation with delamination location through thickness is investigated.

According to Fig. 10, if the delaminated segments are far from the mid-plane the effect of CNTs are more considerable. As an example, for ($h_2 = 0.125h$) adding only 4% CNTs yield 43% improvement of flutter pressure of delaminated nano-composite beam-plates. While for ($h_2 =$

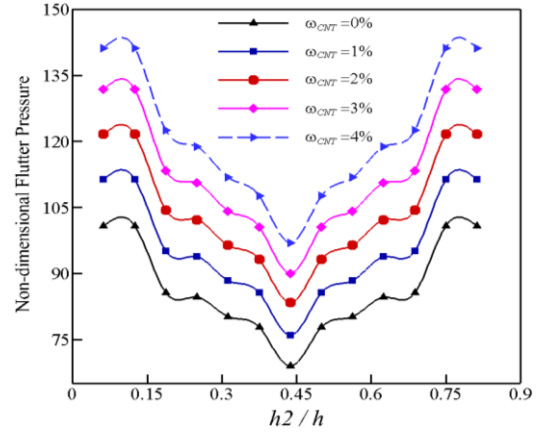


Fig. 11 Effect of delamination position through thickness on flutter pressure of delaminated quasi-isotropic beam-plate with double delamination reinforced with CNTs $(90/\pm 45/0)_{2S}$ ($h_3/h = 1/16$, $d/L = 0.3$, $c/L = 0.5$)

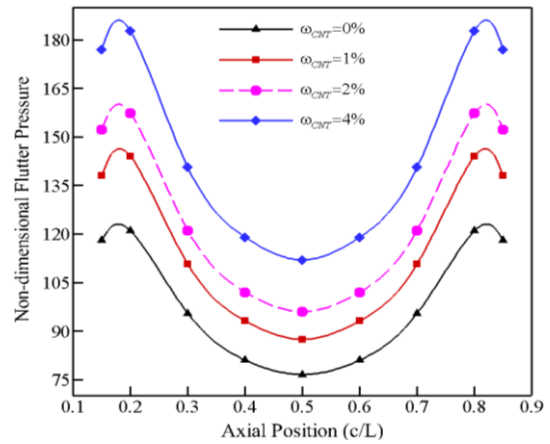


Fig. 12 Effect of delamination axial position on flutter pressure of CNTs reinforced cross-ply beam-plates with double delaminations $(0/90)_S$ ($h_3 = h_4 = 0.25h$, $c/L = 0.5$, $d/L = 0.3$)

0.375h) this growth is less than 30%. A similar behavior can be seen in Fig. 11. According to this figure for ($h_2 = 0.4375h$) adding 1 and 4 percent CNTs can result 10% and 40% improvement of flutter pressure of delaminated nano-composite beam-plates. Fig. 12 depicted the effect of CNTs on flutter pressure variation with delamination axial position. According to the results, if the delamination axial position moves from the mid-span to the edges of beam-plates the effect of CNTs on flutter pressure decreases. In other words, the CNTs can affect flutter pressure more considerable at the maximum destabilizing point at the mid-span in comparison to the axial position farther from the mid-span region.

4. Conclusions

In this paper aeroelastic behavior of 3-phase nano-composite delaminated beam-plate with double delamina-

tions is investigated. CNTs are used to improve mechanical properties of composite beam-plates. The Mori-Tanaka model is used to obtain mechanical properties of CNTs reinforced nano-composite beam-plates. It is assumed that the beam-plate has two delaminations with the same length. Moreover, it is assumed that the delaminated segments are forced to vibrate with each other. Based on the results obtained, CNTs can improve 42% critical flutter boundary of composite delaminated beam-plates at the maximum destabilizing situation while the delamination axial point locates at mid-span. Additionally, it should be noted that adding only 4% CNTs into polymer matrix of symmetric cross-ply (0/90)_s composite beam-plate can shift the frequency coalescences to modes 2 and 4 while for neat epoxy it may occurs for modes 1 and 2. It is important to note that for delaminated beam-plates with two delaminations if the delaminated segments move toward the surface layer of beam-plates flutter pressure is increased while if they approach to the mid-plane result flutter pressure reduction.

References

- Alidoost, H., and Rezaeepazhand, J. (2017), Instability of a delaminated composite beam subjected to a concentrated follower force", *Thin-Wall. Struct.*, **120**, 191-202. <https://doi.org/10.1016/j.tws.2017.08.032>
- Gojny, F.H., Wichmann, M.H.G., Kopke, U., Fiedler, B. and Schulte, B. (2004), "Carbon nanotube-reinforced epoxy-composites: Enhanced stiffness and fracture toughness at low nanotube content", *Compos. Sci. Technol.*, **64**, 2363-2371. <https://doi.org/10.1016/j.compscitech.2004.04.002>
- He, X.Q., Rafiee, M., Mareishi, S. and Liew, K.M. (2015), "Large amplitude vibration of fractionally damped viscoelastic CNTs/fiber/polymer multiscale composite beams", *Compos. Struct.*, **131**, 1111-1123. <https://doi.org/10.1016/j.compstruct.2015.06.038>
- Hu, Y.G., Liew, K.M. and Wang, Q. (2012), "Modeling of vibrations of carbon nanotubes", *Procedia Eng.*, **31**, 343-347. <https://doi.org/10.1016/j.proeng.2012.01.1034>
- Kepple, K.L., Sanborn, G.P., Lacasse, P.A., Gruenberg, K.M. and Ready, W.J. (2008), "Improved fracture toughness of carbon fiber composite functionalized with multi walled carbon nanotubes", *Carbon*, **46**, 2026-2033. <https://doi.org/10.1016/j.carbon.2008.08.010>
- Kharazan, M., Sadr, M.H. and Kiani, M. (2014), "Delamination growth analysis in composite laminates subjected to low velocity impact", *Steel Compos. Struct., Int. J.*, **17**(4), 387-403. <https://doi.org/10.12989/scs.2014.17.4.387>
- Kim, M.G., Hong, J.S., Kang, S.G. and Kim, C.G. (2008), "Enhancement of the crack growth resistance of a carbon/epoxy composite by adding multi-walled carbon nanotubes at a cryogenic temperature", *Compos. Part A: Appl. Sci. Manuf.*, **39**, 647-654. <https://doi.org/10.1016/j.compositesa.2007.07.017>
- Mehar, K. and Panda, S.K. (2016), "Free vibration and bending behaviour of CNT reinforced composite plate using different shear deformation theory", *IOP Conference Series: Materials Science and Engineering*, **115**, 012014. <https://doi.org/10.1088/1757-899X/115/1/012014>
- Murugan, S., Ganguli, R. and Harursampath, D. (2012), "Aeroelastic response of composite helicopter rotor with random material properties", *J. Aircraft*, **45**(1), 306-322. <https://doi.org/10.2514/1.30180>
- Ozdemir, N.G., Zhang, T., Aspin, I., Scaropa, F., Hadavinia, F.H. and Song, Y. (2016), "Toughening of carbon fibre reinforced polymer composites with rubber nanoparticles for advanced industrial applications", *Express Polym. Lett.*, **10**, 394-407. <https://doi.org/10.3144/expresspolymlett.2016.37>
- Rafiee, M., He, X.Q. and Liew, K.M. (2014a), "Nonlinear analysis of piezoelectric nano-composite energy harvesting plates", *Smart Mater. Struct.*, **23**, 065001. <https://doi.org/10.1088/0964-1726/23/6/065001>
- Rafiee, M., Liu, X.F., He, X.Q. and Kitipornchai, S. (2014b), "Geometrically nonlinear free vibration of shear deformable piezoelectric carbon nanotube/fiber/polymer multiscale laminated composite plates", *J. Sound Vib.*, **333**, 3236-3251. <https://doi.org/10.1016/j.jsv.2014.02.033>
- Rafiee, M., Nitzsche, F. and Labrosse, M. (2016), "Rotating nano-composite thin-walled beams undergoing large deformation", *Compos. Struct.*, **150**, 191-199. <https://doi.org/10.1016/j.compstruct.2016.05.014>
- Rafiee, M., Nitzsche, F. and Labrosse, M. (2017), "Dynamics, vibration and control of rotating composite beams and blades: A critical review", *Thin-Wall. Struct.*, **119**, 795-819. <https://doi.org/10.1016/j.tws.2017.06.018>
- Ribeiro, P. (2016), "Non-local effects on the non-linear modes of vibration of carbon nano-tubes under electrostatic actuation", *Int. J. Non-Linear Mech.*, **87**, 1-20. <https://doi.org/10.1016/j.ijnonlinmec.2016.07.007>
- Rizov, V.I. (2017), "Non-linear study of mode II delamination fracture in functionally graded beams", *Steel Compos. Struct., Int. J.*, **23**(3), 263-271. <https://doi.org/10.12989/scs.2017.23.3.263>
- Seidi, J. and Kamarian, S. (2017), "Free vibrations of non-uniform CNT/fiber/polymer nano-composite beams", *Curved Layer Struct.*, **4**, 21-30. <https://doi.org/10.1515/cls-2017-0003>
- Shishesaz, M., Kharazi, M., Hosseini, P. and Hosseini, M. (2017), "Buckling behavior of composite plates with a pre-central circular delamination defect under in-plane uniaxial compression", *J. Computat. Appl. Mech.*, **48**(1), 111-122. <https://doi.org/10.22059/jcamed.2017.234593.147>
- Shi, Z., Yao, Z., Pang, F. and Wang, Q. (2017), "An exact solution for the free-vibration analysis of functionally graded carbon-nanotube-reinforced composite beams with arbitrary boundary conditions", *Scientific Reports*, **7**, 12909. <https://doi.org/10.1038/s41598-017-12596-w>
- Tornabene, F., Baccocchi, M., Fantuzzi, N. and Reddy, J.N. (2017), "Multiscale approach for three-phase CNT/polymer/fiber laminated nano-composite structures", *Polym. Compos.*, **40**(S1), E102-E126. <https://doi.org/10.1002/pc.24520>
- Tracy, J.J. and Pardo, G.C. (1989), "Effect of delamination on the natural frequencies of composite laminates", *J. Compos. Mater.*, **23**, 1200-1215. <https://doi.org/10.1177/002199838902301201>
- Tsantalis, S., Karapappas, P., Vavouliotis, A., Tsotra, P., Kostopoulos, V., Tanimoto, T. and Friedrich, K. (2007), "On the improvement of toughness of cfrps with resin doped with cnf and pzt particles", *Compos. Part A: Appl. Sci. Manuf.*, **38**(4), 1159-1162. <https://doi.org/10.1016/j.compositesa.2006.04.016>
- Yazdi, A.A. (2012), "Flutter of delaminated cross-ply laminated cylindrical shells", *Compos. Struct.*, **94**, 2888-2894. <https://doi.org/10.1016/j.compstruct.2012.03.042>
- Yazdi, A.A. and Rezaeepazhand, J. (2013), "Applicability of small-scale models in prediction flutter pressure of delaminated composite beam plates", *Int. J. Damage Mech.*, **22**(4), 590-601. <https://doi.org/10.1177/1056789512456318>
- Zhang, L.W., Lei, Z.X. and Liew, K.M. (2017), "Free vibration analysis of FG-CNT reinforced composite straight-sided quadrilateral plates resting on elastic foundations using the IMLS-Ritz method", *J. Vib. Control*, **23**(6), 1026-1043. <https://doi.org/10.1177/1077546315587804>

- Zheng, N., Huang, Y., Liu, H.Y., Gao, J. and Mai, Y.W. (2017), "Improvement of interlaminar fracture toughness in carbon fiber/epoxy composites with carbon nanotubes/polysulfone interleaves", *Compos. Sci. Technol.*, **140**, 8-15.
<https://doi.org/10.1016/j.compscitech.2016.12.017>
- Zemirline, A., Ouali, M., and Mahieddine, A. (2015), "Dynamic behavior of piezoelectric bimorph beams with a delamination zone", *Steel Compos. Struct., Int. J.*, **19**(3), 759-776.
<https://doi.org/10.12989/scs.2015.19.3.759>